SIMULATION OF THE FULL COUPLING BETWEEN THE RADIATION TRANSFER AND THE AERODYNAMICS FOR HYPERSONIC REENTRY PROBES

T-H Nguyen-Bui*, J. Dubois
****C.E.A./CESTA, 33114, Le Barp, France,**
ngoc-thanh-ha.nguyen-bui@cea.fr

Keywords: *Radiatif transfer, hypersonic probe*

Abstract

One of the most important parameters for design and one of the most difficult to calculate numerically is the heat transfer to the spacecraft. The heat transfer is composed of two parts: convective and radiative heating. In effect, a very intense shock wave, created at the front of atmospheric reentry vehicles during their flight, leads the temperature behind the shock to raise up to several thousand degrees. As a consequence, the sizing of the thermal protection system (TPS) is a crucial step in the preliminary design study of a probe.
The calculation of a flow around a reentry vehicle involves many parameters that make necessary the use of robust codes. The present work concerns the use of the M_1 model for radiative transfer fully coupled with aerodynamics equations. The numerical simulations around the space probes are performed and presented in this paper.

1 Introduction

A very intense shock wave is created at the front of atmospheric reentry vehicles during their flight. Almost all the kinetic energy changes into internal and chemical energy. The temperature raises behind the shock up to several thousand degrees.
It mainly deals with controlled reentry of vehicles which are intended to reach the planetary surface intact, although it may also include minimally controlled cases such as destructive deorbiting of satellites. Typically, this reentry process requires special methods to protect against aerodynamic heating. Indeed, depending on the entry parameters, the effects can be very different. For instance, in the case of a space shuttle coming back to Earth, the conditions are such that radiation plays only a neglectable part compared to the hydrodynamic effects. Meanwhile, in some cases, radiative transfer is determinant.
And finally, the velocity of a superorbital object entering the atmosphere can be very high. Indeed, the objective of such high speed reentries is to save fuel by slowing down the vehicle only using the planet's atmosphere as an aerodynamic brake. As an example, for the returning Appolo capsules, two third of the energy was dissipated by the means of radiative transfer effects.
A discussion about the optimum shape of an entry vehicle [1] concludes that a body of large nose radius is favorable in planetary entries as it produces a thick shock layer. This observation was the basic principle on which were built the early space missions vehicles. However, such a shape revealed to bring an unexpected heating related to radiation. As a matter of fact, the temperature in the shock layer being very high (of the order of 10000K), the gas is then fully dissociated, or partially ionised, and it also leads to the production of radiation. This phenomenon, amongst the chemical and aerodynamic phenomena, is thus taken into account in nowadays feasibility studies of atmospheric reentry.

The calculation of a flow around a reentry vehicle involves many parameters that make necessary the use of robust codes. Indeed, considering radiative transfer, we must be able to approximate closely enough the solution of the radiative transfer equation in regimes as different as the diffusion regime in the hot and dense gases of the shock layer, and the transport regime in the cold and transparent regions, as well as the intermediate regimes. The medium opacities are determined from the chemical composition of the gas and the state the species are in, some radiating more or less, and depending on the temperature range the database may not be complete. Moreover, the hydrodynamic behaviour of the flow should not be neglected as it dictates the position and characteristics of the shock and the drag, and can be influenced by the radiative effects.

The present work concerns the use of the M_1 model for radiative transfer fully coupled with aerodynamics equations. We developed an accurate finite volume method according to the nonlinear system of conservation laws that governs this model. We proposed to derive an HLLC method which preserves the stationary contact waves. To supplement this essential property, the method is proved to be robust and to preserve the physical admissible states. A relevant asymptotic preserving correction is proposed in order to obtain a method which is able to deal with all the physical regimes [2]. The model M_1 is next introduced into an aerothermodynamic software in order to simulation the flow around a hypersonic probe fully coupled with the radiation transfer.

2 Mathematical Modeling

2.1 Governed Equations

Let us consider the conservative balance equations for mass fraction for ne chemical species, momentum, and total energy.

$$\frac{\partial \rho C_\alpha}{\partial t} + \frac{\partial \rho u_j C_\alpha}{\partial x_j} = \frac{\partial}{\partial x_j}\left(\rho D_\alpha \frac{\partial C_\alpha}{\partial x_j}\right) + \dot{\omega}_\alpha \tag{1}$$

$$\begin{aligned}&\frac{\partial \rho u_i}{\partial t} + \frac{\partial \rho u_j u_i}{\partial x_j} = -\frac{\partial p}{\partial x_i} + F_i \\ &+ \frac{\partial}{\partial x_j}\left[\mu\left(\frac{\partial u_i}{\partial x_j} + \frac{\partial u_j}{\partial x_i} - \frac{2}{3}\frac{\partial u_l}{\partial x_l}\delta_{ij}\right)\right]\end{aligned} \tag{2}$$

$$\begin{aligned}&\frac{\partial \rho E}{\partial t} + \frac{\partial \rho u_j E}{\partial x_j} = -\frac{\partial p u_i}{\partial x_i} + F_j u_j \\ &+ \frac{\partial}{\partial x_i}\left(\lambda \frac{\partial T}{\partial x_i}\right) + \frac{\partial}{\partial x_j}\left(\tau_{ij} u_i\right) \\ &+ \frac{\partial}{\partial x_i}\left(\sum_1^{n_e} \rho D_\alpha h_\alpha \frac{\partial C_\alpha}{\partial x_i}\right) - \dot{q}_R\end{aligned} \tag{3}$$

2.2 Radiative transfer

The radiative transfer phenomenon is involved in many applications and its relevant numerical simulation turns out to be essential. Solving the full radiative transfer equation is in general too expansive, and alternative model must be considered.

2.2.1 Description

Let us assume the Radiative Transfer Equation (RTE) with no scattering source term, and a frozen flow in Local Thermal Equilibrium. In fact, radiative transfer is not conserved so we choose to couple the radaitive and matters energies to obtain a conserved total energy. We describe radiative transfer and its interaction with matter through the following equations:

$$\begin{aligned}&\frac{1}{c}\frac{\partial I}{\partial t} + \vec{\Omega}.\vec{\nabla} I = \sigma(B_\nu(T) - I) \\ &\frac{\partial \rho C_v T}{\partial t} = -\int_0^{+\infty}\int_{S^2} \sigma(B_\nu(T) - I) d\Omega d\nu\end{aligned} \tag{4}$$

where T is the matter temperature, ρ is the density, and C_v is the specific heat at the constant volume. The term $\sigma(B_\nu(T) - I)$ sets a balance between the photons emission and absorption opacity ($B_\nu(T)$ is the Planck's function at the frequency ν).

Let us emphasize that the radiative equations (5) and (6), issued from the first two moments of the radiative transfer equation, are coupled to the matter, involving the temperature T governed by equation (7).

$$\partial_t E + \nabla \cdot \mathbf{F} = c\sigma\big(aT^4 - E\big), \qquad (5)$$

$$\partial_t \mathbf{F} + c^2\, \nabla \cdot \mathbf{P} = -c\sigma\ \mathbf{F}, \qquad (6)$$

$$\partial_t(\rho\ C_v T) = -c\sigma\big(aT^4 - E\big). \qquad (7)$$

Here, *E* denotes the radiative energy and *F* the radiative flux vector. The positive constants *c* and σ respectively denote the speed of light and the opacity. The positive constant *a* is prescribed by physics.
From this system, there exist many possibilities in the choice of the closure hypothesis. This choice is indeed important as it determines the various properties of the model, its capacities and failures.

2.2.2 M_1 Model

In recent years, several models have been introduced and the present work is devoted to one of them; namely the M_1 model introduced by Dubroca-Feugeas [7]. This model is able to restore some essential physical properties satisfied by the radiation transfer equation. Indeed, this model provides an accurate prediction of radiation and matter interaction. In addition, both energy positiveness and flux limitation are preserved. An other important property restored by the model concerns an asymptotic diffusive regime which is reached as soon as the opacities are larger (see Mihalas-Mihalas [14] or Pomraning [15]).
Also, we introduce the Eddington factor χ, in ordre to express the radiative pressure ***P***, it is given by:

$$\mathbf{P} = \frac{1}{2}\left((1-\chi(f))\mathbf{I} + (3\chi(f)-1)\frac{\mathbf{F}\otimes\mathbf{F}}{||\mathbf{F}||^2}\right)E \qquad (8)$$

with

$$\chi(f) = \frac{3+4f^2}{5+2\xi}, \quad \xi = \sqrt{4-3f^2}$$

where we have introduced the normalized flux vector ***f***=***F***/*cE* and we have set *f*=||***f***||.

The interest of the M_1 model is twofold. On one hand, it preserves the positiveness of the radiative energy, ($E \geq 0$) and the flux limitation, $f \leq 1$. On the other hand, the suggested model satisfies an equilibrium diffusion regime when the opacity tends to infinity (see [14], [15]). Indeed, as soon as σ is large, we introduce a rescaling factor ε, a Knudsen number like, to rewrite the system as follows:

$$\begin{cases} \epsilon\partial_t E + \ \nabla\cdot\mathbf{F} = \frac{c\sigma}{\epsilon}(aT^4 - E) \\ \epsilon\partial_t F + \ c^2\nabla\cdot\mathbf{F} = -\frac{c\sigma}{\epsilon}F, \\ \epsilon\partial_t(\rho C_v T) = -\frac{c\sigma}{\epsilon}(aT^4 - E). \end{cases} \qquad (9)$$

Arguing a classic Chapman-Enskog expansion where ε, the equilibrium state is defined by $E_0 = aT_0^4$ and $F_0 = 0$ while the equilibrium temperature is solution of the following diffusion equation:

$$\partial_t(\rho C_v T_0 + aT_0^4) - \nabla\cdot\left(\frac{c}{3\sigma}\nabla T_0^4\right) = 0 \qquad (10)$$

3 Numerical Methods

3.1 Software

The numerical methods presented in this document have been introduced in the ARES code from the CEA/CESTA. ARES is a two dimensional aerothermodynamic code that contains various types of flow models such as Euler, Navier-Stokes, and with turbulence models, simple chemistry or non-equilibrium chemistry. This code is based on an extension of Roe's approximate Riemann solver [17]. The Harten-Yee TVD scheme [11] is used to solve the hyperbolic part of Navier-Stokes equations. The second order of spatial precision is obtained using minmod limiter. The Navier-Stokes equations is strongly coupled with radiation transfer equations. This coupling is taken into account through the source terms.

3.2 Numerical Consideraion of the M_1 Model

The first approach of the M_1 model was developed by [7] where an HLL scheme was proposed. This scheme was robust since it preserved the admissible states. Unfortunately such a numerical approach failed to approximate the asymptotic diffusion behaviour. To correct such an issue, several techniques were proposed in the litterature and the reader is refered to Gosse-Toscani [10], Buet-Cordier [5], Buet-Després [6], Berthon *et al.* [2], [4] for a description of the main numerical methods. In fact, all these techniques are the same strategy. The first step is devoted to the transport operator given by:

$$\begin{cases} \partial_t E + \nabla \cdot \mathbf{F} = 0, \\ \partial_t \mathbf{F} + c^2 \nabla \cdot \mathbf{P} = 0 \\ \partial_t (\rho C_v T) = 0, \end{cases} \tag{11}$$

where a standard HLL scheme (see [12] for the details) is considered. The main benefit of this numerical approximation is an easy preservation of the admissible states for a viscous discretisation. Actually, the difference between all the above mentionned works concerns the numerical process of the resolution.
The main comment about this very brief overview concerns the approximation of the transport part of the M_1 model, given by (Eq. 11), which is systematically approximated by the well-known HLL numerical procedure. Indeed, as soon as σ is set equal to zero, all the above cited numerical methods turn out to coincide with the explicit or implicit HLL scheme for (Eq. 11).
Recently we developped a new numerical scheme [3]. That is to derive a contact preserving scheme [18] of the HLLC type to approximate the weak solution of (Eq. 11). Such an accuracy property is useful to perform simulations of physical interest. We proved that the updated radiation state vector remains admissible with a positive radiative energy and a relevant flux limitation [3].

4 Numerical Results

4.1 Shadow cone

Let us now consider a 2D academic test case. It has very stiff initial conditions and intends to demonstrate the quality of the solution provided by the solver. Tests have been performed in [2], and we show here some improvements from the results obtained therein.
We consider the domain (x, y)∈[0, 2] × [0, 1]m as shown on Fig. 4. Computations made here are run on a 80 × 40 cartesian grid, with a time step Δt fixed by the CFL restriction. The domain is composed of a dense material (ρC_v=8.6 × 10^4 $Jm^{-3}K^{-1}$ and σ=2 × $10^5 m^{-1}$) and a transparent region. A free streaming beam adjacent to the dense material enters the domain through the top left boundary. The other boundaries of the domain are supposed to be transparent. The initial temperature is 1K in the dense material and 300K elsewhere. A radiative temperature of T=5.8×10^6K is applied on the left side of the transparent region (from *y*=0.5m to *y*=1m).

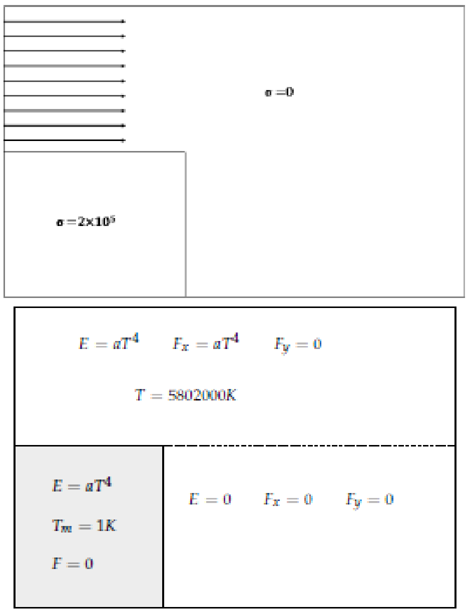

Fig. 1: Geometry (left) and exact solution (right) for the 2D case.

The exact solution is drawn on Fig. 1. Indeed, in the upper part the photons are simply translated from the left boundary to the right of the domain. In the lower part, the solution remains constant against time since no photon enters this area. The line *y*=0.5m is then a stationary contact discontinuity for the M_1-system. The dense material does not get any photon either and its temperature remains constant.

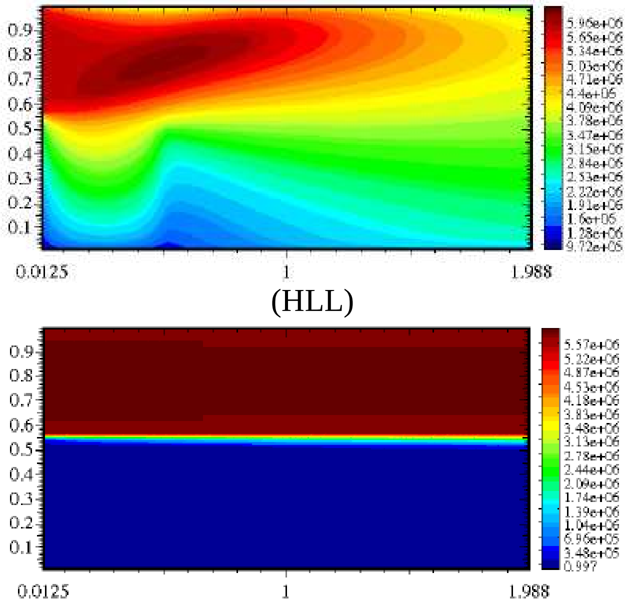

(HLL)

(HLLC)

Fig. 2: Comparison of the radiative temperature predicted by the HLL scheme (top) with the HLLC (buttom).

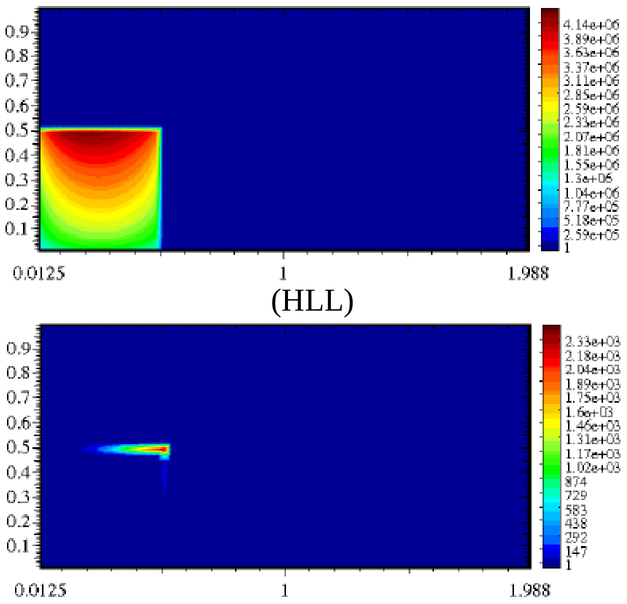

(HLL)

(HLLC)

Fig. 3: Comparison of the material temperature computed by the HLL scheme (top) with the HLLC (buttom).

Simulations are stopped at time t=5 $\times$ 10^{-8}s. Figs. 2 and 3 respectively show the radiative and material temperature distributions obtained from the HLL and HLLC schemes. It is obvious that the HLL scheme induces an important numerical diffusion which affects the lower part of the domain. On the other hand, the HLLC scheme is able to deal properly with the discontinuity. Solution of the HLLC scheme with the asymptotic preserving correction and a second order MUSCL extension has a behavior very close to the exact solution.

4.2 Venusian Atmospheric Reentry

We have here performed simulations of a hypersonic flow around a planetary reentry probe in the case of a Venus like reentry.

In this numerical experiment, we look at an object with the dimensions of the Pioneer Venus bus portion of the spacecraft that reached Venus in December 1978. It is a 2.5m diameter vehicle weighing 250kg. The trajectory point considered in this simulation is located at an altitude of about 80km, and the temperature at this point is of 142K and the pressure is 300Pa. Atmospheric reentries in Venus are to be known to be quite difficult because of the thickness of its atmosphere (about 90 times thicker than the Earth atmosphere). For the simulations performed here, we solely look at the forepart of the body.

The chemical composition of the venusian atmosphere is assumed to be made of 100% of CO_2. The initial opacities are also considered constant over the computed domain and equal to $5000 m^{-1}$.

The chemical species considered in the calculations are CO_2, CO, C, C_2, O_2.

We can observe that the flow is entirely modified. The shock positions are differents for the two simulations (11 cm at the axis when the RT is not taken into account, against 3.7 cm for the case coupled) (Fig. 4 and Fig. 5).

Additionally, we refine the mesh in the boundary layer close to the body. This second mesh is still divided into 40 cells in the x direction and 15 cells in the y direction, as the original mesh, but is refined on the boundary of the probe. Fig. 6 shows the temperature predicted on the two different meshes by both HLL and HLLC schemes.

We can see that the HLLC scheme predicts similar results on both grids while the solution of the HLL scheme contains much more numerical diffusion on the first grid.

We thus confirm the gain in accuracy we have made when developing an HLLC like Riemann solver. Moreover, from a computation cost point of view, performing these tests on one processor (type: Itanium II - 1.6 GHz), we outline that it is approximately two times longer to obtain a converged solution with the refined mesh than with the regular mesh. It is therefore cheaper to realize the needed calculations over a regular mesh, and it is accurate enough when using the HLLC approximate Riemann solver.

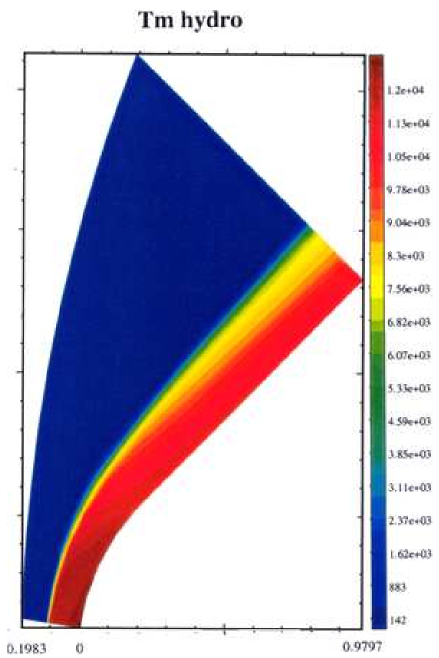

Fig.4 : Isotherme (simulation without Transfer Radiative coupling)

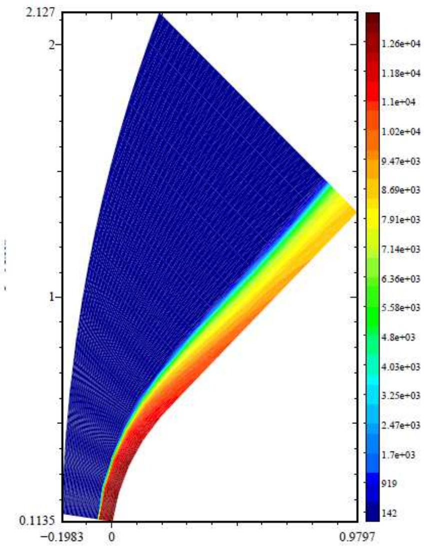

Fig. 5 Isothermes (simulation with Transfer Radiative coupling)

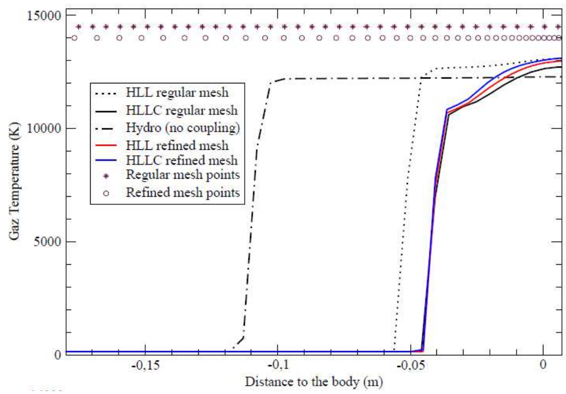

Fig. 6: Center line Temperature Distributions (comparison "no coupling" and with coupling)

4.3 Flight Case : FIRE II

The Fire II mission took place in May 22nd, 1965. The FIRE-II flight experiment was performed in 1965 in order to validate the aerothermodynamic models used to design the Apollo thermal protection system. Its main goal was the assessment of the radiative heating environment during an Earth reentry. The vehicle geometry was an Apollo type with a reentry velocity of 11.4 km/s.

The case simulated is a point of the trajectory at 1636s, taken at the Altitude = 71.04km (Earth atmosphere).

The geometry 93.47 cm radius Sphere is considered.

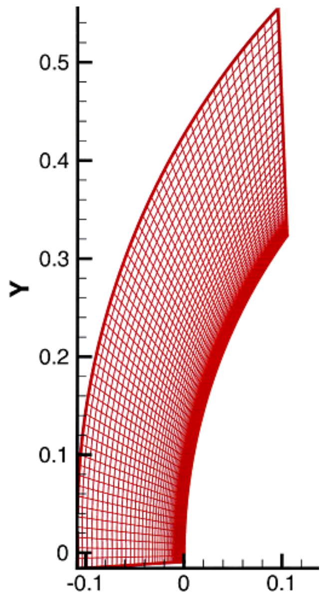

Fig. 7: 60 * 100 Mesh
V=11.4 km.s^{-1}, Density = 8.57×10^{-5} kg.m^{-3}, T_∞=210 K, T_w = 810 K

The case is simulated with MonoTemperature T. 11 species (N_2, O_2, NO, N, O, N_2+, N+, O_2+, O+, NO+, e-) are considered and Park chemical kinetic reactions (20 chemical reactions with catalicity) [1] are included for calculation.

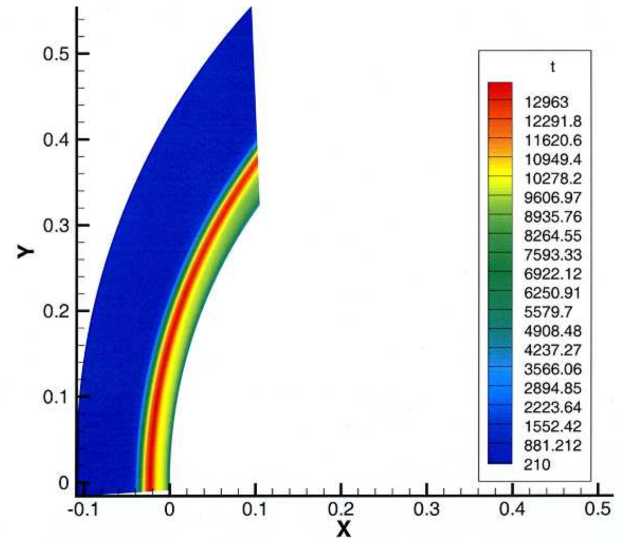

Fig. 8: Isotherm around the FIRE-II spacecraft Strong Coupling with Radiative Transfer

A general overview of the flowfield is presented in Fig. 8, which shows contours of translational temperature in the flowfield.

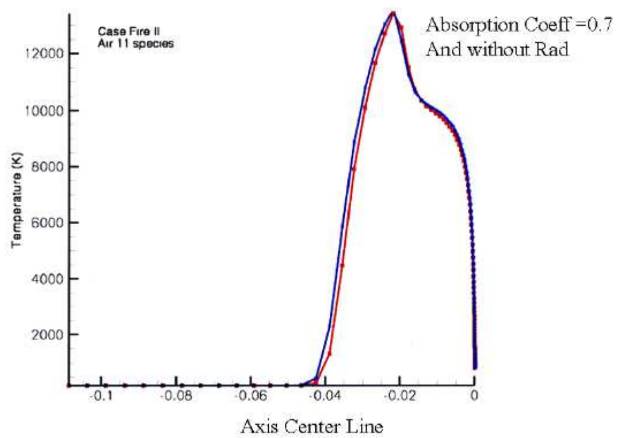

Fig. 9 : Temperature profiles along the stagnation line for the 1636 seconds, 11-species, noncatalytic wall case.

The temperature profiles are concordants with other studies [19]. For this case of the reentry of FIRE II into the Earth atmosphere, its influence on the radiative heat flux is negligible

5 Conclusions

A code for the simulation of hypersonic flows at reentry conditions is developed. This code allows us to take into account the radiative transfer thank to a strong coupling between the aerodynamics part and the radiative transfer. The use of the new numerical technique ensures a judicious discretization of the source term and preserves a discrete limit diffusion equation. Several numerical experiments attest the relevance of the method and its ability to perform simulations of physical interest.

In the future, we will develop the method multigroup in order to take into account the variation of the opacity in function of the frequency and the temperature.

References

[1] C. Park, “Overview of radiation problems in planetary entries”, *Procedings of the International Workshop on Radiation of High Temperature Gases in Atmospheric. Entry*, ESA SP-583, May 2005.

[2] C. Berthon, J. Dubois, R. Turpault, *Numerical Approximation of the M1 Model*, Edition SMF, Panoramas et Synthèses 28, 2009

[3] C. Berthon, J. Dubois, T.-H. Nguyen-Bui, and R. Turpault, A free Streaming Contact Preserving Scheme for the M1 Model, *Advances in Applied Mathematics and Mechanics*, Volume 2, Numero 3, ISSN: 2070-0733, June 2010

[4] C. Berthon, P. Charrier, B. Dubroca, An HLLC. Scheme to Solve the M1 Model of Radiative Transfer in Two Space Dimensions , *J. Sci. Comput.*, Vol 31, 2007

[5] C. Buet, S. Cordier, Asymptotic Preserving Scheme and Numerical Methods for Radiative Hydrodynamic Models, *C.R.Acad.Sci. Paris, Tome 338* (2004), Série I, 951-956

[6] C. Buet, B. Després, Asymptotic Analysis of Fluid Models for the Coupling of Radiation and Hydrodynamics, *J. Quant. Spectrosc. Radiat. Transfer*, 85 (2004), 3-4, 385-418

[7] B. Dubroca, J.-L. Feugeas, Hierarchie de Modeles aux Moments pour le Transfert Radiatif, *C.R.Acad.Sci. Paris*, tome 329, 1999, Serie I, pp 915-920

[8] C.A.J. Fletcher, *Computational Techniques for Fluid Dynamics - Specific Techniques for Different Flow Categories*, Springer-Verlag, Vol.2, 1988

[9] M. Gonzalez, *Contribution à l'étude numérique de l'hydrodynamique radiative: des expériences de chocs radiatifs aux jets astrophysiques*, PhD Report Université Paris-Sud XI, Oct. 2006

[10] L. Gosse, G. Toscani, Asymptotic-Preserving Well-Balanced Scheme for the Hyperbolic Heat Equations, *C.R.Acad.Sci. Paris*, tome 334 (2002), Série I, 337-342

[11] A. Harten, P.D. Lax, B. van Leer, On Upstream Di_erencing and Godunov-Type Schemes for Hyperbolic Conservation Laws, *SIAM Review*, Vol.25, No.1, January 1983

[12] Harten A., Warming R.F., Yee H.C. “Implicit Total Variation Diminishing Schemes for Steady States Calculating”, *AIAA paper 83-1902*, 1983.

[13] J.C. Hayes & M.L. Norman, Beyond Flux-Limited Di_usion: Parallel Algorithms for Multidimensional Radiation Hydrodynamics, *ApJS*, 147:197-220, July 2003

[14] D. Mihalas, G. W. Mihalas, *Foundation of Radiation Hydrodynamics*, Oxford University Press, 1984

[15] G.C. Pomraning, *The Equations of Radiation Hydrodynamics*, Sciences Application, 1973

[16] S. Richling, E. Meinköhn, N. Kryzhevoi and G. Kanschat, Radiative Transfer with Finite Elements. I. Basic method and tests, *A&A*, 452:907-920, June 2001

[17] Roe P.L., Approximate Riemann Solvers, Parameter Vectors and Difference Schemes, J. *Comput. Phys*., Vol 43, 1982.

[18] E.F. Toro, *Riemann Solvers and Numerical Methods for Fluid Dynamics - A Practical Introduction*, Springer-Verlag Berlin Heidelberg, 1999

[19] L. C. Scalabrin, I. D. Boyd, Numerical Simulations of the FIRE-II Convective and Radiative Heating Rates, *AIAA 2007-4044*, 2007

Copyright Statement